J. Fluid Mech. (2000), *vol.* 414, *pp.* 315–337. Printed in the United Kingdom

Destabilization of a vortex by acoustic waves

By STÉPHANE LEBLANC

Department of Mathematics, University of Toulon and Var BP 132,
F-83957 La Garde Cedex, France

(Received 26 July 1999 and in revised form 16 February 2000)

The linear stability of a circular vortex interacting with two plane acoustic waves propagating in opposite directions is investigated. When the wavelength is large compared to the size of the vortex, the core is subjected to time-periodic compressions and strains. A stability analysis is performed with the geometrical optics approximation, which considers short-wavelength perturbations evolving along the trajectories of the basic flow. On the vortex core, the problem is reduced to a single Hill–Schrödinger equation with periodic or almost-periodic potential, the solution to which grows exponentially when parametric resonances occur. On interacting with the acoustic waves, the circular vortex is thus unstable to three-dimensional perturbations.

1. Introduction

Hydrodynamic instabilities in compressible flows remain relatively not well understood for at least two reasons: first because only few equilibrium basic-state solutions of the equations of motion are known, and secondly because the perturbation problem is more difficult than in the incompressible case, as it involves an additional equation. Furthermore, as in the incompressible case, most of the hydrodynamic stability theories concern basic flows with relatively simple topology and some particular symmetries, allowing simplification of the spectral problem (Drazin & Reid 1981; Saffman 1992; Huerre & Rossi 1998).

Nevertheless, the theory of short-wavelength perturbations in inviscid flows provides a powerful tool for linear stability of complex flows. There has been significant progress with the fundamental works of Eckhoff (1981) and Lifschitz & Hameiri (1991), who proposed a method based on the WKB approximation which allows local stability criteria to be derived for any incompressible or compressible time-dependent flows (see also Dobrokhotov & Shafarevich 1992; Vishik & Friedlander 1993). Instead of characterizing the discrete eigenmodes with large wavenumbers (Moore & Saffman 1975; Tsai & Widnall 1976; Leibovich & Stewartson 1983; Bayly 1988; Le Duc & Leblanc 1999; Eloy & Le Dizès 2000; Sipp & Jacquin 2000) or constructing localized solutions corresponding to the continuous spectrum (Lifschitz 1991; Lebovitz & Lifschitz 1992) as performed in ideal magnetohydrodynamics (see Lifschitz 1989), the *geometrical optics stability theory* of Eckhoff (1981) and Lifschitz & Hameiri (1991) consists in solving the initial value problem corresponding to localized initial data. By expanding the solution in a WKB form, the linearized Euler equations are reduced to a system of ordinary differential equations evolving along the trajectories of the basic flow. As in geometrical optics, this system consists of the eikonal equation for the wave vector and the transport equations for the perturbation amplitude, which may be solved often analytically, otherwise by an elementary numerical integration. An unbounded solution of the transport equations is sufficient to prove instability.

The geometrical optics stability theory is now a standard tool, and in incompressible flows, the results are numerous. Let us mention some applications to centrifugal-type instabilities (Bayly 1988; Lifschitz & Hameiri 1993; Sipp & Jacquin 2000), stagnation points (Friedlander & Vishik 1991; Lifschitz & Hameiri 1991; Leblanc 1997), chaotic flows (Friedlander & Vishik 1992; Lifschitz 1994; Reyl, Antonsen & Ott 1997), strained vortices (Bayly, Holm & Lifschitz 1996; Sipp & Jacquin 1998; Le Dizès & Eloy 1999), finite-amplitude waves (Fabijonas, Holm & Lifschitz 1997; Miyazaki & Adachi 1998), or rotating flows (Lebovitz & Lifschitz 1996; Leblanc & Cambon 1998; Sipp, Lauga & Jacquin 1999; Le Dizès 2000*b*). This list of references is not exhaustive.

Less is known on the stability of compressible flows, except for steady basic states with circular symmetry. With a normal mode approach, Gans (1975), Warren (1975) and Lalas (1975) derived necessary conditions for instability. With the short-wavelength approximation, Eckhoff & Storesletten (1978, 1980) derived sufficient instability criteria, extending considerably Rayleigh's criterion for centrifugal instability and anticipating the incompressible result of Leibovich & Stewartson (1983) for vortex breakdown (see the discussion in Eckhoff 1984). Lebovitz & Lifschitz (1992) studied localized instabilities in rotating fluid masses with both a description of the continuous spectrum and the geometrical optics method. Le Duc & Leblanc (1999) gave the asymptotic structure of the unstable eigenmodes with large axial wavenumbers for the compressible Rayleigh criterion. For steady flows with complex topology, Lifschitz & Hameiri (1991) showed that any steady subsonic flow of a compressible ideal gas having a non-degenerate point of stagnation is unstable unless this point lies on the axis of rigid body rotation. In other words, it means that any elliptical vortex core or hyperbolic stagnation point is locally unstable; for instance, the compressible Hill's spherical vortex (Moore & Pullin 1998) is linearly unstable. On the other hand, any circular vortex core in a steady flow is locally stable. Complementary to inertial modes, acoustic modes may also be responsible for instability (Broadbent & Moore 1979) or algebraic transient growth (Chagelishvili *et al.* 1997; Simone, Coleman & Cambon 1997).

In time-dependent compressible flows at low Mach number, Mansour & Lundgren (1990) and Leblanc & Le Penven (1999) found parametric instabilities in unbounded circular or elliptical vortices that were periodically compressed. Although these time-periodic compressible flows are not physically realistic, an interesting question is whether they could mimic the behaviour of a smooth localized vortex interacting with a long-wavelength acoustic wave.† Since the works of Kraichnan (1953) and Lighthill (1953), it is known that sound propagation is modified by turbulence and vortical flows (see also Landau & Lifshitz 1959). Acoustic waves are also used to excite, with loudspeakers, instabilities in mixing layers or jets (see for instance Ho & Huerre 1984). Recently, Lund & Rojas (1989) proposed a method using ultrasound to characterize a turbulent flow, and various experimental techniques have been proposed (Dernoncourt, Pinton & Fauve 1998; Labbé & Pinton 1998; Oljaca *et al.* 1998; Manneville *et al.* 1999).

Scattering of sound waves by a smooth circular vortex has also been studied analytically and numerically (Colonius, Lele & Moin 1994; Reinschke, Möhring & Obermeier 1997). In a recent work, Ford & Llewellyn Smith (1999) performed an asymptotic analysis of wave scattering by a vortex, and gave a detailed description of the flow in both outer and inner regions, corresponding respectively to the wave and the vortical region. Their solution, derived in the Born limit, i.e. the wavelength is

† This question was raised by an anonymous referee of Leblanc & Le Penven (1999).

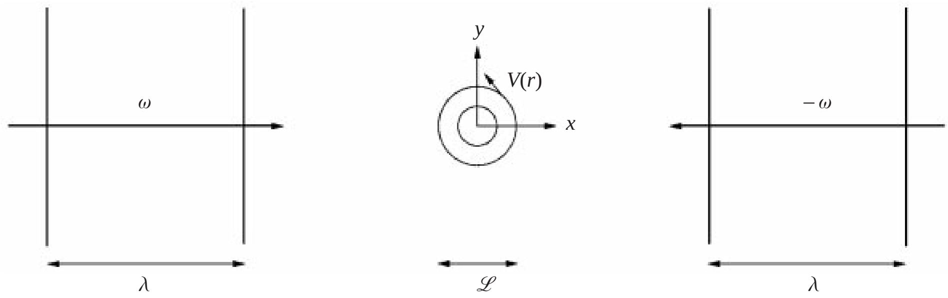

FIGURE 1. Sketch of a circular vortex of characteristic size $\mathscr{L}$ and velocity distribution $V(r)$, interacting with two acoustic waves with wavelength λ, and pulsation $\pm\omega$. The Born limit corresponds to $\lambda \gg \mathscr{L}$.

large compared to the size of the vortex, is in good agreement with direct numerical simulations of Colonius *et al.* (1994). Their results will help us to give a partial answer to the problem posed above: the superposition of two acoustic waves with opposite directions of propagation (figure 1) may destabilize a vortex, by compressing and straining periodically the vortex core.

The paper is organized as follows: in § 2, the geometrical optics stability theory is recalled, and it is shown how to reduce the problem to a single Hill–Schrödinger equation. Some illustrative effects of local compressions and strains on vortex cores are analysed in § 3, and a complete description of the corresponding parametric resonances is given. Section 4 details the destabilization of circular vortices by a pair of acoustic waves, and the results are applied to a Rankine vortex.

2. The geometrical optics stability theory

2.1. *Basic equations*

Let $[\boldsymbol{U}, R, P](\boldsymbol{x}, t)$ be the velocity, density and pressure fields of the subsonic compressible flow of an ideal gas filling a domain $\mathscr{D}_t$ bounded or not. The flow is governed by the compressible Euler equations:

$$\frac{\mathrm{D}R}{\mathrm{D}t} + R\nabla\cdot\boldsymbol{U} = 0, \qquad \frac{\mathrm{D}\boldsymbol{U}}{\mathrm{D}t} + \frac{1}{R}\nabla P = 0, \qquad \frac{\mathrm{D}P}{\mathrm{D}t} + \gamma P\nabla\cdot\boldsymbol{U} = 0, \tag{2.1}$$

where $\gamma > 1$ is the constant ratio of specific heats, and $\mathrm{D}/\mathrm{D}t = \partial/\partial t + \boldsymbol{U}\cdot\nabla$ is the material derivative. The last equation for pressure is deduced from entropy conservation $\mathrm{D}S/\mathrm{D}t = 0$, with $S = P/R^{\gamma}$ for a perfect gas. When $\mathscr{D}_t$ is bounded, the flow is subject to slip boundary conditions for the velocity field.

Let $\mathscr{U}$, $\mathscr{R}$, $\mathscr{P}$, $\mathscr{L}$ and $\mathscr{T}$ denote respectively some characteristic velocity, density, pressure, length and time scales of the flow, and let $[\boldsymbol{U}', R', P'](\boldsymbol{x}', t')$ denote the corresponding dimensionless variables. Clearly, the ratio between the convective time scale $\mathscr{L}/\mathscr{U}$ and the natural time scale $\mathscr{T}$ defines a Strouhal number that appears in the dimensionless equations. Here, we assume that the Strouhal number is of order unity, so that unsteady terms balance convective ones. Dropping the primes, the dimensionless Euler equations are

$$\frac{\mathrm{D}R}{\mathrm{D}t} + R\nabla\cdot\boldsymbol{U} = 0, \tag{2.2}$$

$$\frac{\mathrm{D}\boldsymbol{U}}{\mathrm{D}t}+\frac{\nabla P}{\gamma \mathscr{M}^2 R}=0, \tag{2.3}$$

$$\frac{\mathrm{D}P}{\mathrm{D}t}+\gamma P\nabla\cdot\boldsymbol{U}=0, \tag{2.4}$$

where $\mathscr{M}=\mathscr{U}/\mathscr{C}$ is the characteristic Mach number of the flow, and $\mathscr{C}=\sqrt{\gamma\mathscr{P}/\mathscr{R}}$ its characteristic sound celerity.

Taking the curl of the momentum equation (2.3), the dimensionless compressible Helmholtz equation for the vorticity $\boldsymbol{W}=\nabla\times\boldsymbol{U}$ is (Saffman 1992)

$$\frac{\mathrm{D}}{\mathrm{D}t}\left(\frac{\boldsymbol{W}}{R}\right)=\boldsymbol{L}\left(\frac{\boldsymbol{W}}{R}\right)+\frac{\nabla R\times\nabla P}{\gamma\mathscr{M}^2R^3}, \tag{2.5}$$

where the tensor $\boldsymbol{L}$ is defined by $\boldsymbol{L}=\nabla\boldsymbol{U}$.

2.2. *Short-wavelength perturbations*

Adding a small perturbation $[\boldsymbol{u},\varrho,p](\boldsymbol{x},t)$ to the basic flow described by $[\boldsymbol{U},R,P](\boldsymbol{x},t)$, injecting into Euler equations, and neglecting nonlinear terms yields a linear system of differential equations, that may be rewritten by using Eckart's dimensionless variables $[m,n](\boldsymbol{x},t)$ defined by (Eckhoff & Storesletten 1978)

$$\varrho=\mathscr{M}\frac{R}{C}(m+n),\quad p=\gamma\mathscr{M}RCn, \tag{2.6}$$

where $C=\sqrt{P/R}$ is the dimensionless local sound celerity of the basic flow.

In terms of Eckart's variables, the linear dimensionless system is

$$\frac{\mathrm{D}\boldsymbol{u}}{\mathrm{D}t}+\boldsymbol{L}\,\boldsymbol{u}+\frac{C}{\mathscr{M}}\left(-\frac{\nabla P}{\gamma P}m+\nabla n+(\gamma-1)\frac{\nabla P}{\gamma P}n-\frac{\nabla C}{C}n\right)=0, \tag{2.7}$$

$$\frac{\mathrm{D}m}{\mathrm{D}t}+(\gamma-1)\frac{\mathrm{tr}\,\boldsymbol{L}}{2}m+\frac{C}{\mathscr{M}}\left(\frac{\nabla R}{R}-\frac{\nabla P}{\gamma P}\right)\cdot\boldsymbol{u}=0, \tag{2.8}$$

$$\frac{\mathrm{D}n}{\mathrm{D}t}+(\gamma-1)\frac{\mathrm{tr}\,\boldsymbol{L}}{2}n+\frac{C}{\mathscr{M}}\left(\nabla\cdot\boldsymbol{u}+\frac{\nabla P}{\gamma P}\cdot\boldsymbol{u}\right)=0, \tag{2.9}$$

where $\mathrm{D}/\mathrm{D}t=\partial/\partial t+\boldsymbol{U}\cdot\nabla$ is the material derivative following the basic flow, $\boldsymbol{L}=\nabla\boldsymbol{U}$ is the basic velocity gradient tensor which verifies: $\mathrm{tr}\,\boldsymbol{L}=\nabla\cdot\boldsymbol{U}$.

Following Eckhoff (1981) and Lifschitz & Hameiri (1991), we seek an asymptotic solution of the linear system of the WKB (Wentzel–Kramers–Brillouin) form:

$$[\boldsymbol{u},m,n](\boldsymbol{x},t)=\mathrm{e}^{\mathrm{i}\phi(\boldsymbol{x},t)/\varepsilon}[\tilde{\boldsymbol{u}},\tilde{m},0](\boldsymbol{x},t)+O(\varepsilon), \tag{2.10}$$

where ϕ is a real-valued phase field and $\varepsilon\ll 1$ is a small real parameter at our disposal. Injecting (2.10) into (2.7), (2.8) and (2.9), and equating the various orders in ε yields, at leading order $O(1/\varepsilon)$: $\mathrm{D}\phi/\mathrm{D}t=0$ and $\boldsymbol{k}\cdot\tilde{\boldsymbol{u}}=0$, where $\boldsymbol{k}=\nabla\phi$ is the wave vector. Advection of ϕ gives

$$\frac{\mathrm{D}\boldsymbol{k}}{\mathrm{D}t}=-\boldsymbol{L}^T\boldsymbol{k}, \tag{2.11}$$

where ^{T} stands for transpose.

At $O(1)$, (2.7) and (2.8) give respectively

$$\frac{\mathrm{D}\tilde{\boldsymbol{u}}}{\mathrm{D}t}=\left(\frac{2\boldsymbol{k}\boldsymbol{k}^T}{|\boldsymbol{k}|^2}-\boldsymbol{I}\right)\boldsymbol{L}\,\tilde{\boldsymbol{u}}+\frac{C}{\mathscr{M}}\left(\boldsymbol{I}-\frac{\boldsymbol{k}\boldsymbol{k}^T}{|\boldsymbol{k}|^2}\right)\frac{\nabla P}{\gamma P}\tilde{m}, \tag{2.12}$$

$$\frac{\mathrm{D}\tilde{m}}{\mathrm{D}t} = (1-\gamma)\frac{\mathrm{tr}\,\boldsymbol{L}}{2}\tilde{m} + \frac{C}{\mathscr{M}}\left(\frac{\nabla P}{\gamma P} - \frac{\nabla R}{R}\right)\cdot\tilde{\boldsymbol{u}}. \tag{2.13}$$

Higher-order corrections to (2.10) may be computed (Lifschitz & Hameiri 1991).

2.3. *Lagrangian description*

Equations (2.11), (2.12) and (2.13) involve only a material derivative following the basic flow $\mathrm{D}/\mathrm{D}t$. Using a Lagrangian representation $\boldsymbol{x} = \boldsymbol{x}(\boldsymbol{X}, t)$, where $\boldsymbol{X} = \boldsymbol{x}(\boldsymbol{X}, 0)$, and introducing the trajectories of the basic flow, the system of partial differential equations (2.11), (2.12) and (2.13) is transformed into a system of *ordinary* differential equations evolving along the trajectories (Lifschitz & Hameiri 1991). Before this, we define $[\boldsymbol{a}, b](\boldsymbol{X}, t)$ as

$$\boldsymbol{a} = \sqrt{J}\tilde{\boldsymbol{u}}, \quad b = \sqrt{J}\tilde{m}, \tag{2.14}$$

where $J(\boldsymbol{X}, t) = \det(\partial\boldsymbol{x}/\partial\boldsymbol{X})$ is the solution of $\mathrm{d}J/\mathrm{d}t = J\nabla\cdot\boldsymbol{U}$ with $J(\boldsymbol{X}, 0) = 1$.

The complete system of ordinary differential equations is then

$$\frac{\mathrm{d}\boldsymbol{x}}{\mathrm{d}t} = \boldsymbol{U}, \tag{2.15}$$

$$\frac{\mathrm{d}\boldsymbol{k}}{\mathrm{d}t} = -\boldsymbol{L}^T\boldsymbol{k}, \tag{2.16}$$

$$\frac{\mathrm{d}\boldsymbol{a}}{\mathrm{d}t} = \left(\frac{2\boldsymbol{k}\boldsymbol{k}^T}{|\boldsymbol{k}|^2} - \boldsymbol{I}\right)\boldsymbol{L}\,\boldsymbol{a} + \frac{\mathrm{tr}\,\boldsymbol{L}}{2}\boldsymbol{a} + \frac{C}{\mathscr{M}}\left(\boldsymbol{I} - \frac{\boldsymbol{k}\boldsymbol{k}^T}{|\boldsymbol{k}|^2}\right)\frac{\nabla P}{\gamma P}b, \tag{2.17}$$

$$\frac{\mathrm{d}b}{\mathrm{d}t} = \frac{C}{\mathscr{M}}\left(\frac{\nabla P}{\gamma P} - \frac{\nabla R}{R}\right)\cdot\boldsymbol{a} + (2-\gamma)\frac{\mathrm{tr}\,\boldsymbol{L}}{2}b. \tag{2.18}$$

In the geometrical optics approximation, (2.15) corresponds to the equation of rays, which are trajectories in the present case, (2.16) is the eikonal (or Hamilton–Jacobi) equation, whereas (2.17) and (2.18) are the transport (or Liouville) equations. Initial conditions $[\boldsymbol{k}, \boldsymbol{a}, b](\boldsymbol{X}, 0)$ may be constructed such that $\boldsymbol{k}(\boldsymbol{X}, 0)\cdot\boldsymbol{a}(\boldsymbol{X}, 0) = 0$, ensuring $\boldsymbol{k}\cdot\boldsymbol{a} = 0$ at any time (Lifschitz & Hameiri 1991).

As proved by Eckhoff (1981) and Lifschitz & Hameiri (1991), *a sufficient condition for instability* is the unbounded growth of $|\boldsymbol{a}(\boldsymbol{X}, t)|$ or $|b(\boldsymbol{X}, t)|$ along a given trajectory $\boldsymbol{X}$.

2.4. *Reduction to a Hill–Schrödinger equation*

We are particularly interested in the stability of unsteady vortices for which the core position $\boldsymbol{x}_0$ is *steady* in the frame of reference, i.e. such that $\boldsymbol{U}(\boldsymbol{x}_0, t) = 0$. Such points are stagnation points, and are particular trajectories of the basic flow, for which $\mathrm{d}\boldsymbol{x}_0/\mathrm{d}t = 0$. At the stagnation point, acceleration is zero since $\mathrm{d}^2\boldsymbol{x}_0/\mathrm{d}t^2 = 0$, so that the momentum conservation equation (2.3) gives, at the stagnation point,

$$\nabla P = 0, \tag{2.19}$$

whereas mass (2.2) and entropy (2.4) conservations give respectively

$$\frac{1}{R}\frac{\mathrm{d}R}{\mathrm{d}t} = \frac{1}{\gamma P}\frac{\mathrm{d}P}{\mathrm{d}t} = -\mathrm{tr}\,\boldsymbol{L}, \tag{2.20}$$

since $\mathrm{tr}\,\boldsymbol{L} = \nabla\cdot\boldsymbol{U}$.

Now, suppose that the basic flow is planar and two-dimensional in the plane $(\boldsymbol{e}_x, \boldsymbol{e}_y)$. Let $\boldsymbol{L}$ denote now the local 2×2 velocity gradient tensor. The basic vorticity $W\boldsymbol{e}_z$ is a solution of the two-dimensional compressible Helmholtz equation which is on $\boldsymbol{x}_0$, from (2.5) and (2.19),

$$\frac{\mathrm{d}}{\mathrm{d}t}\left(\frac{W}{R}\right) = 0. \tag{2.21}$$

As done by Bayly *et al.* (1996) for an incompressible flow, let us now show that the study of the transport equations (2.17) and (2.18) at $\boldsymbol{x}_0$ may be reduced to a single Hill–Schrödinger equation. Let ξ and $\boldsymbol{v}$ denote respectively the projection of the wave vector $\boldsymbol{k}$ and of the amplitude $\boldsymbol{a}$ on the $(\boldsymbol{e}_x, \boldsymbol{e}_y)$-plane, and $\mu = \boldsymbol{k} \cdot \boldsymbol{e}_z$. Let $\boldsymbol{H}$ be the 2×2 tensor defined by

$$\boldsymbol{H} = \boldsymbol{L}\begin{pmatrix} 0 & 1 \\ -1 & 0 \end{pmatrix}. \tag{2.22}$$

Assuming that $\xi \neq 0$ and $\mu \neq 0$, we introduce the new variables

$$p = \frac{|\boldsymbol{k}|}{|\xi|}\sqrt{R}\,\xi \cdot \boldsymbol{v}, \quad q = \frac{|\boldsymbol{k}|}{|\xi|}\frac{\boldsymbol{k} \times \boldsymbol{a}}{\sqrt{R}} \cdot \boldsymbol{e}_z. \tag{2.23}$$

After some manipulations, we get the following system of ordinary differential equations:

$$\frac{\mathrm{d}p}{\mathrm{d}t} = \left(\frac{\mathrm{d}}{\mathrm{d}t}\ln\frac{|\xi|}{|\boldsymbol{k}|}\right)p + \left(\frac{2R\mu^2}{|\xi|^2|\boldsymbol{k}|^2}\xi^T\boldsymbol{H}\xi\right)q, \tag{2.24}$$

$$\frac{\mathrm{d}q}{\mathrm{d}t} = -\left(\frac{W}{R}\right)p - \left(\frac{\mathrm{d}}{\mathrm{d}t}\ln\frac{|\xi|}{|\boldsymbol{k}|}\right)q. \tag{2.25}$$

Taking the time derivative (2.25) and taking into account (2.21) and (2.24), we get the following Hill–Schrödinger equation:

$$\frac{\mathrm{d}^2q}{\mathrm{d}t^2} + Q(\boldsymbol{x}_0, t)q = 0, \tag{2.26}$$

where the potential $Q(\boldsymbol{x}_0, t)$ is similar to the incompressible case (Bayly *et al.* 1996):

$$Q(\boldsymbol{x}_0, t) = \frac{2W\mu^2}{|\xi|^2|\boldsymbol{k}|^2}\xi^T\boldsymbol{H}\xi + \frac{\mathrm{d}^2}{\mathrm{d}t^2}\ln\frac{|\xi|}{|\boldsymbol{k}|} - \left(\frac{\mathrm{d}}{\mathrm{d}t}\ln\frac{|\xi|}{|\boldsymbol{k}|}\right)^2. \tag{2.27}$$

It may be verified that when $R(\boldsymbol{x}_0, t)$, $|\xi(\boldsymbol{x}_0, t)|$ and $|\boldsymbol{k}(\boldsymbol{x}_0, t)|$ are bounded in time (which is generally the case in vortex cores), the unbounded growth of $|q(\boldsymbol{x}_0, t)|$ is sufficient for instability. As mentioned before, $q(\boldsymbol{x}_0, t)$ is not defined when $\mu = 0$, but this case corresponds to two-dimensional short-wavelength perturbations, that may be shown to be stable when $|\boldsymbol{k}(\boldsymbol{x}_0, t)|$ is bounded.

In planar homentropic flows, entropy is spatially uniform so that (2.4) is replaced by $P = R^\gamma$. Linearization yields $p = \gamma C^2 \varrho$, so that $m = 0$ and $b = 0$. The immediate consequence is that the Hill–Schrödinger equation (2.26) with (2.27) is valid on *any* trajectory $\boldsymbol{X}$ (and not only at a stagnation point $\boldsymbol{x}_0$).

3. Illustrative examples of parametric resonances

3.1. *Circular compressions*

Before proceeding to the core of the paper, i.e. the stability analysis of the interaction between a circular vortex and acoustic waves, it is useful to illustrate the basic mechanisms of instability by some explicit examples. For a given planar flow with stagnation point $\boldsymbol{x}_0$, we see from (2.21) that $W(\boldsymbol{x}_0, t)$ and $R(\boldsymbol{x}_0, t)$ are proportional;

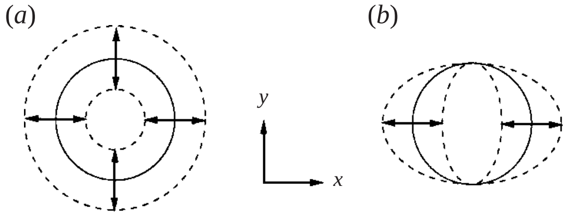

FIGURE 2. Sketch of the local flows near the vortex cores for circular (*a*) and axial (*b*) compressions: streamline of the steady vortex cores (solid lines) and envelopes of the trajectories in the time-periodic case (dashed lines).

we chose $W(\boldsymbol{x}_0, t) = R(\boldsymbol{x}_0, t)$. We give now some local solutions that satisfy the local equilibrium constraint (2.20) and for which the eikonal equation (2.11) admits exact solutions.

The local velocity gradient tensor,

$$\boldsymbol{L}(\boldsymbol{x}_0, t) = \frac{1}{2}\begin{pmatrix} -\dfrac{1}{R}\dfrac{\mathrm{d}R}{\mathrm{d}t} & -R \\ R & -\dfrac{1}{R}\dfrac{\mathrm{d}R}{\mathrm{d}t} \end{pmatrix}, \tag{3.1}$$

satisfies (2.20) and (2.21) by construction, so that it is a local solution of the equations of motion. Assuming the periodic compressions

$$R(\boldsymbol{x}_0, t) = 1 + \delta\cos(\omega t), \tag{3.2}$$

with pulsation $\omega > 0$ and amplitude $0 \leqslant \delta < 1$, the flow corresponds locally to a circular vortex core subjected to isotropic *circular* compressions in the $(\boldsymbol{e}_x, \boldsymbol{e}_y)$-plane (figure 2).

With (3.1), the eikonal equation admits the following solution:

$$\boldsymbol{k}(\boldsymbol{x}_0, t) = \left(\sqrt{1-\mu^2}\sqrt{R}\cos\tau,\ \sqrt{1-\mu^2}\sqrt{R}\sin\tau,\ \mu\right)^T, \quad \tau(t) = \int_0^t \frac{R}{2}\,\mathrm{d}t, \tag{3.3}$$

where $0 \leqslant \mu \leqslant 1$ characterizes the three-dimensionality of the perturbation: when $\mu = 0$, the perturbation is planar and two-dimensional since $\boldsymbol{k}\cdot\boldsymbol{a} = 0$; otherwise it is three-dimensional. Thus, the short-wavelength stability problem is partially solved. It remains to characterize the large-time behaviour of the solution the Hill–Schrödinger equation (2.26). This is performed below for weak amplitudes.

Indeed, when $\delta \ll 1$, the local velocity gradient tensor (3.1), may be expanded in powers of δ as

$$\boldsymbol{L}(\boldsymbol{x}_0, t) = \boldsymbol{L}_0 + \delta\boldsymbol{L}_1(t) + O(\delta^2), \tag{3.4}$$

where

$$\boldsymbol{L}_0 = \frac{1}{2}\begin{pmatrix} 0 & -1 \\ 1 & 0 \end{pmatrix}, \tag{3.5}$$

which corresponds to an unperturbed circular vortex core with unit vorticity, and

$$\boldsymbol{L}_1(t) = \frac{1}{2}\begin{pmatrix} \omega\sin(\omega t) & -\cos(\omega t) \\ \cos(\omega t) & \omega\sin(\omega t) \end{pmatrix}, \tag{3.6}$$

which is a compressible rotational correction.

The corresponding potential in the Hill–Schrödinger equation (2.26) may be explicitly computed and gives, when $\delta \ll 1$,

$$Q(\boldsymbol{x}_0, t) = Q_0 + \delta Q_1(t) + O(\delta^2), \tag{3.7}$$

where $Q_0 = \mu^2$ and

$$Q_1(t) = \mu^2 \left(\mu^2 + 1 - \frac{\omega^2}{2} \right) \cos(\omega t). \tag{3.8}$$

When $\delta = 0$ (no compression), the Hill–Schrödinger equation (2.26) admits an exact solution for $q(\boldsymbol{x}_0, t)$ which is periodic in time with pulsation μ, so that the steady circular vortex core is stable, in accordance with Lifschitz & Hameiri (1991). Nevertheless, it is worth noting that these local periodic short waves correspond in fact to Kelvin waves propagating inside the vortex, and we will see that weak compressions and/or strains may be responsible for parametric resonances.

3.2. *A Mathieu equation*

Thus, for pure circular compressions, (2.26) is (at order δ)

$$\frac{\mathrm{d}^2 q}{\mathrm{d}t^2} + \mu^2 \left\{ 1 + \delta \left(\mu^2 + 1 - \frac{\omega^2}{2} \right) \cos(\omega t) \right\} q = 0, \tag{3.9}$$

which may be recognized as a standard Mathieu equation (Magnus & Winkler 1966; Bender & Orszag 1978), the prototype of the parametric resonance equation. To order δ, corresponding solutions are periodic and stable (bounded), except near

$$|\mu| = \frac{|\omega|}{2}, \tag{3.10}$$

which corresponds to the first parametric resonance of the Mathieu equation. Since $0 < \mu < 1$ and $\omega > 0$, we expect instability when

$$0 < \omega < 2. \tag{3.11}$$

A standard multiple-scale asymptotic analysis (Bender & Orszag 1978) may be carried out in order to characterize the first resonance (3.10); we omit the analysis here because it is completely standard. Near (3.10), the most unstable solution is

$$q(\boldsymbol{x}_0, t) = q_0 \exp \left\{ \frac{\omega}{8} \left(1 - \frac{\omega^2}{4} \right) \delta t \right\} \cos \left(\frac{\omega t}{2} + \phi_0 \right) + O(\delta), \tag{3.12}$$

where q_0 and ϕ_0 are some initial constants. Since $0 < \mu < 1$, the first parametric resonance occurs as expected when $0 < \omega < 2$. The cases $\mu = 0$ (two-dimensional perturbations) and $\mu = 1$ are stable.

3.3. *Axial compressions*

Let us now turn to a more complex situation where the vortex is compressed along a given axis (say $\boldsymbol{e}_x$). As previously, it may be verified that the flow described locally by

$$\boldsymbol{L}(\boldsymbol{x}_0, t) = \begin{pmatrix} -\dfrac{1}{R}\dfrac{\mathrm{d}R}{\mathrm{d}t} & -\dfrac{\Omega}{R} \\ \Omega R & 0 \end{pmatrix}, \quad \Omega(t) = \frac{R^2}{R^2 + 1}, \tag{3.13}$$

verifies the local equilibrium constraints (2.20) and (2.21). With periodic compressions given by (3.2), the flow corresponds to a vortex core with locally circular streamlines when $\delta = 0$ (no compression), and otherwise, as represented on figure 2, trajectories are inscribed into two elliptical envelopes, so that it is a circular vortex core which is *axially* compressed along the $\boldsymbol{e}_x$-axis.

Once again, the eikonal equation may be locally solved (Leblanc & Le Penven 1999):

$$\boldsymbol{k}(\boldsymbol{x}_0, t) = \left(\sqrt{1-\mu^2}R\cos\tau,\ \sqrt{1-\mu^2}\sin\tau,\ \mu\right)^T, \quad \tau(t) = \int_0^t \Omega\,\mathrm{d}t. \tag{3.14}$$

For arbitrary amplitudes of compressions, $\delta \sim O(1)$, the solution of (2.26) may be studied numerically with Floquet theory when $Q(\boldsymbol{x}_0, t)$ is periodic or with a Prufer transformation when $Q(\boldsymbol{x}_0, t)$ is almost periodic (Craik & Allen 1992; Bayly *et al.* 1996; Leblanc & Le Penven 1999), but no definitive theorems exist to characterize the stability characteristics of such Hill–Schrödinger equations, except tests for stability (Magnus & Winkler 1966).

When $\delta \ll 1$, the local velocity gradient (3.13) is

$$\boldsymbol{L}(\boldsymbol{x}_0, t) = \boldsymbol{L}_0 + \delta\boldsymbol{L}_1(t) + O(\delta^2), \tag{3.15}$$

where $\boldsymbol{L}_0$ is given by (3.5), and

$$\boldsymbol{L}_1(t) = \frac{1}{2}\begin{pmatrix} \omega\sin(\omega t) & -\cos(\omega t) \\ \cos(\omega t) & \omega\sin(\omega t) \end{pmatrix} + \frac{1}{2}\begin{pmatrix} \omega\sin(\omega t) & \cos(\omega t) \\ \cos(\omega t) & -\omega\sin(\omega t) \end{pmatrix}. \tag{3.16}$$

The first term in the right-hand side corresponds to the compressible rotational correction (3.6). The second term is a pure incompressible irrotational correction: it may be related to a time-periodic straining field studied numerically by Bayly *et al.* (1996).

The potential of the Hill–Schrödinger equation is, after some algebra,

$$Q(\boldsymbol{x}_0, t) = Q_0 + \delta Q_1(t) + O(\delta^2), \tag{3.17}$$

where $Q_0 = \mu^2$ as before, and

$$\begin{aligned} Q_1(t) = {} & \mu^2\left(\mu^2 + 1 - \frac{\omega^2}{2}\right)\cos(\omega t) + \mu^2\left(\frac{\mu^2}{2} - \frac{\omega^2+5}{4} - \omega\right)\cos(1+\omega)t \\ & +\mu^2\left(\frac{\mu^2}{2} - \frac{\omega^2+5}{4} + \omega\right)\cos(1-\omega)t. \end{aligned} \tag{3.18}$$

We see from the above formula that the first term of the right-hand side corresponds to (3.8), i.e. to a pure compressible effect, whereas the remaining terms are related to the irrotational incompressible straining field.

3.4. *Almost-periodic potentials*

Now when $\delta \ll 1$, the stability analysis of the vortex compressed axially is reduced to (at order δ)

$$\frac{\mathrm{d}^2 q}{\mathrm{d}t^2} + \{Q_0 + \delta Q_1(t)\}q = 0, \tag{3.19}$$

where $Q_0 = \mu^2$ and $Q_1(t)$ is given by (3.18). This case requires a careful analysis. Indeed, $Q_1(t)$ is either periodic (when ω is a rational number), or almost periodic (when ω is irrational). Thus, the resulting equation is no longer a Mathieu equation. Fortunately, the principal resonances may be studied with a multiple-scale analysis.

For small amplitudes, Craik & Allen (1992) obtained a similar equation for time-periodic incompressible linear flows, and argued that each forcing term in the potential

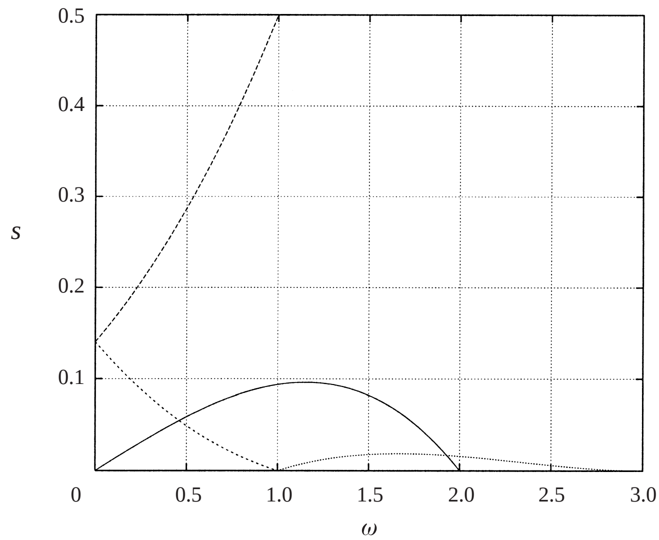

FIGURE 3. Rescaled growth rates $s = \sigma/\delta$ of the various principal parametric instabilities in the case of axial compressions given by expressions (3.22), (3.23) and (3.24). The resonance defined when $0 < \omega < 2$ (solid line) also corresponds to the case of circular compressions.

(3.18) is responsible for a region of instability centred on half its frequency. In short, it means that three different resonances arise from

$$|\mu| = \frac{|\omega|}{2}, \quad |\mu| = \frac{|1+\omega|}{2}, \quad |\mu| = \frac{|1-\omega|}{2}. \tag{3.20}$$

Since $0 < \mu < 1$ and $\omega > 0$, this means that the leading-order parametric instabilities cannot happen unless

$$0 < \omega < 3. \tag{3.21}$$

However, this qualitative argument gives no indication on the growth rates. So we use multiple-scale asymptotics to characterize precisely the three parametric instabilities. Furthermore, various resonances may interact for some particular values of the parameters. Details of the calculations are given in Appendix A and the results may be summarized as follows (to order δ).

The resonance $\omega = 2\mu$ happens when $0 < \omega < 2$, and the perturbation grows exponentially with growth rate

$$\sigma = \frac{\delta\omega}{8}\left(1 - \frac{\omega^2}{4}\right), \tag{3.22}$$

exactly as for the circular compressions. The resonances $1 \pm \omega = 2\mu$ both happen when $0 < \omega < 1$ with respective growth rates:

$$\sigma = \frac{\delta}{64}(1 \pm \omega)(3 \pm \omega)^2. \tag{3.23}$$

The resonance $\omega - 1 = 2\mu$ happens for $1 < \omega < 3$, and the corresponding growth rate is

$$\sigma = \frac{\delta}{64}(\omega - 1)(\omega - 3)^2. \tag{3.24}$$

These resonances are plotted in figure 3. Some particular cases may arise when two of these bandwidths interact. These correspond to $\omega = \frac{1}{2}$ or $\omega = 1$ with some particular orientations μ of the wave vector, and they are analysed in detail in Appendix A. However, they do not affect the most unstable perturbations. Finally, as noted previously, two-dimensional perturbations ($\mu = 0$) are stable, whereas the most unstable configuration is reached for spanwise wave vectors ($\mu = 1$) with

$$\omega = 1, \ \sigma = \delta/2. \tag{3.25}$$

These results complete the description of the resonances at weak amplitude obtained numerically by Leblanc & Le Penven (1999) for a compressed vortex at low Mach number.

To conclude, it is worth mentioning that in an incompressible flow, the resonances of a circular vortex which experiences weak periodic irrotational strains may be deduced from the above results: resonances correspond to (3.23) and (3.24).

4. Destabilization of a circular vortex by acoustic waves

4.1. *The scattering of a wave by a circular vortex*

Since time-periodic compressions are responsible for three-dimensional parametric instabilities in a steady vortex core, it is natural to ask whether an acoustic wave may destabilize a vortex. The interaction of sound waves with a vortex, i.e. the *scattering* of waves by a vortical region, is a classical problem in aeroacoustic theory: when a single plane wave travels along the $\boldsymbol{e}_x$-axis in the positive x-direction and propagates through a vortical region, the acoustic field is significantly modified, and the far field has been characterized successfully both numerically and analytically (Colonius *et al.* 1994; Reinschke *et al.* 1997; Ford & Llewellyn Smith 1999).

When the wavelength λ of the incident acoustic wave is large compared to the characteristic size of the vortex $\mathscr{L}$, i.e. in the Born limit $\lambda \gg \mathscr{L}$, Ford & Llewellyn Smith (1999) gave a description of the resulting flow both in the wave region (the outer region) and in the vortical region (the inner region). Their construction is asymptotically consistent since matching of the flows in the two regions is ensured. Furthermore, their results have been compared successfully to the direct numerical simulations of Colonius *et al.* (1994). In their analysis, the flow is assumed homentropic, with small Mach number $\mathscr{M} = \mathscr{U}/\mathscr{C} \ll 1$, where $\mathscr{U}$ is a characteristic velocity of the vortex, and $\mathscr{C}$ is the sound celerity of waves propagating in a flow at rest. The incident wave is characterized by the wavenumber k and pulsation $\omega = \mathscr{C}k$, which is assumed of the same order as the characteristic time scale of the vortex, i.e. $\omega \sim \mathscr{U}/\mathscr{L} \sim O(1)$. Thus, the Strouhal number $\omega\mathscr{L}/\mathscr{U}$ is assumed to be $O(1)$, so that it may be verified that $\mathscr{L} \sim \mathscr{M}\lambda$.

4.2. *Solution in the vortex region*

Ford & Llewellyn Smith (1999) solved the full compressible Euler equations for an homentropic flow in the inner and outer regions with asymptotic matching, for an incident plane wave with dimensionless amplitude δ. In the vortical region, the dimensionless velocity fields is denoted $\boldsymbol{U}^+(\boldsymbol{x},t)$ (the $^+$ is used to characterize the flow perturbed by a wave propagating in the *positive* x-direction). It is†

$$\boldsymbol{U}^+(\boldsymbol{x},t) = \boldsymbol{U}_0^+(\boldsymbol{x}) + \delta \boldsymbol{U}_1^+(\boldsymbol{x},t) + O(\delta^2), \tag{4.1}$$

† Note that unlike our notation, the flow in the vortical region is described by lowercase letters in Ford & Llewellyn Smith (1999), whereas capital letters were reserved for the outer region. No ambiguity is possible here, since we are only interested in the vortical region.

where

$$\boldsymbol{U}_0^+(\boldsymbol{x}) = V(r)\boldsymbol{e}_\theta = r\Omega(r)\boldsymbol{e}_\theta, \tag{4.2}$$

which corresponds to a circular vortex centred at the origin of the frame. The core vorticity is assumed to be unity (singular point vortices are excluded from the analysis). We assume furthermore that the vortex is stable to three-dimensional compressible centrifugal instabilities (Eckhoff & Storesletten 1978; Le Duc & Leblanc 1999).

The $O(\delta)$ correction is expanded as

$$\boldsymbol{U}_1^+(\boldsymbol{x},t) = \boldsymbol{U}_{01}^+(\boldsymbol{x},t) + \mathscr{M}\boldsymbol{U}_{11}^+(\boldsymbol{x},t) + \mathscr{M}^2\boldsymbol{U}_{21}^+(\boldsymbol{x},t) + O(\mathscr{M}^3 \ln \mathscr{M}), \tag{4.3}$$

where $\boldsymbol{U}_{01}^+$, $\boldsymbol{U}_{11}^+$ and $\boldsymbol{U}_{21}^+$ may be deduced from (3.6 *b*), (3.11), (4.10), (4.14) and (4.16) in Ford & Llewellyn Smith (1999). They are

$$\boldsymbol{U}_{01}^+ = 0, \quad \boldsymbol{U}_{11}^+ = \boldsymbol{e}_z \times \nabla\Psi_{11}^+, \quad \boldsymbol{U}_{21}^+ = \nabla\Phi_{21}^+ + \boldsymbol{e}_z \times \nabla\Psi_{21}^+, \tag{4.4}$$

where

$$\Psi_{11}^+(r,\theta,t) = -r\left(\sin\theta + \mathrm{i}\frac{\Omega}{\omega}\cos\theta\right)\mathrm{e}^{-\mathrm{i}\omega t}, \tag{4.5}$$

$$\Phi_{21}^+(r,\theta,t) = \tfrac{1}{4}\mathrm{i}\omega r^2\mathrm{e}^{-\mathrm{i}\omega t}, \tag{4.6}$$

$$\Psi_{21}^+(r,\theta,t) = \frac{1}{2}\left(r^2\Omega - \frac{\Gamma}{2\pi}\right)\mathrm{e}^{-\mathrm{i}\omega t} + g_{2,\omega}(r)\mathrm{e}^{\mathrm{i}(2\theta-\omega t)} + g_{-2,\omega}(r)\mathrm{e}^{\mathrm{i}(-2\theta-\omega t)}, \tag{4.7}$$

where Γ is the constant total circulation of the vortex, and the functions $g_{n,\omega}(r)$ are solutions of the radial Rayleigh equation:

$$\frac{\mathrm{d}^2}{\mathrm{d}r^2}g_{n,\omega} + \frac{1}{r}\frac{\mathrm{d}}{\mathrm{d}r}g_{n,\omega} - \left(\frac{n^2}{r^2} - \frac{n}{r(\omega - n\Omega)}\frac{\mathrm{d}W}{\mathrm{d}r}\right)g_{n,\omega} = 0, \tag{4.8}$$

which may encounter singular critical layers at radii r_0 where $\omega = n\Omega(r_0)$ (see Drazin & Reid 1981). These singularities may be regularized by viscosity or nonlinearity (Reinschke *et al.* 1997; Le Dizès 2000 *a*). For our purpose, we assume that the critical layers for $n = \pm 2$ (if they exist) are outside the vortex core $r_0 = 0$, i.e.

$$\omega \neq 1, \tag{4.9}$$

since $\Omega = \frac{1}{2}$ at $r = 0$ by assumption (unit vorticity in the core), and $\omega > 0$. Furthermore, according to Ford & Llewellyn Smith (1999), solution (4.7) is no longer valid when ω corresponds to a two-dimensional eigenfrequency of the vortex. Higher-order corrections to (4.3) and expressions for pressure and density may be found in Ford & Llewellyn Smith (1999).

Thus, at $O(\mathscr{M})$, we see that the first effect of the incident wave on the vortex is to move its centre with a time-periodic motion of translation: this may be clearly seen by taking the real part of $\boldsymbol{U}_{11}^+$ expressed at $r = 0$. This gives

$$\boldsymbol{U}_{11}^+(0,\theta,t) = \cos(\omega t)\boldsymbol{e}_x - \frac{1}{2\omega}\sin(\omega t)\boldsymbol{e}_y. \tag{4.10}$$

It will be shown below that the $O(\mathscr{M}^2)$ effect of the acoustic wave is to compress and strain time periodically the vortex core. Nevertheless, the instability mechanisms exposed previously are not valid here, since the position of the vortex core is no longer steady, according to (4.10). Then, by superposing a second acoustic wave propagating along the $\boldsymbol{e}_x$-axis, but with *opposite* direction (figure 1), we may expect that the motion of translation $\boldsymbol{U}_{11}^+$ will be annihilated, so that parametric resonances should occur.

4.3. *The case of two waves*

The analysis of Ford & Llewellyn Smith (1999) could be completely redone when the leading-order solution in the outer wave region is the superposition of a first wave propagating along the $\boldsymbol{e}_x$-axis in the positive x-direction and a second wave propagating along the $\boldsymbol{e}_x$-axis in the negative x-direction. However, this is not necessary since the solution of Ford & Llewellyn Smith (1999) corresponds to the linear correction $O(\delta)$ to the vortex flow. Thus, the simultaneous effects of the two waves on the vortex is simply the sum of the $O(\delta)$ terms of each solution.

Furthermore, the solution corresponding to the wave propagating in the *negative* x-direction may be deduced from the results of Ford & Llewellyn Smith (1999) by using the following transformation for each scalar field:

$$(\omega, k) \to (-\omega, -k), \quad (r, \theta) \to (r, \theta + \pi), \quad (x, y) \to (-x, -y), \tag{4.11}$$

which means simply that the solution for the wave propagating in the negative x-direction is obtained by symmetry with respect to the origin, together with $\omega \to -\omega$.

The leading-order unperturbed circular vortex remains unchanged by this transformation. For the $O(\delta)$ corrections, we get from (4.5), (4.6) and (4.7)

$$\Psi_{11}^{+} \to \Psi_{11}^{-}, \quad \Phi_{21}^{+} \to \Phi_{21}^{-}, \quad \Psi_{21}^{+} \to \Psi_{21}^{-}, \tag{4.12}$$

with

$$\Psi_{11}^{-}(r, \theta, t) = r\left(\sin\theta - \mathrm{i}\frac{\Omega}{\omega}\cos\theta\right)\mathrm{e}^{\mathrm{i}\omega t}, \tag{4.13}$$

$$\Phi_{21}^{-}(r, \theta, t) = -\tfrac{1}{4}\mathrm{i}\omega r^2 \mathrm{e}^{\mathrm{i}\omega t}, \tag{4.14}$$

$$\Psi_{21}^{-}(r, \theta, t) = \frac{1}{2}\left(r^2\Omega - \frac{\Gamma}{2\pi}\right)\mathrm{e}^{\mathrm{i}\omega t} + g_{-2,\omega}(r)\mathrm{e}^{\mathrm{i}(2\theta+\omega t)} + g_{2,\omega}(r)\mathrm{e}^{\mathrm{i}(-2\theta+\omega t)}, \tag{4.15}$$

since from (4.8) it may be verified that $g_{n,-\omega}(r) = g_{-n,\omega}(r)$ providing that they have a similar behaviour when $r \to \infty$, which is the case here (Ford & Llewellyn Smith 1999).

Now, if the two waves have the same amplitude δ, their simultaneous effects on the vortex are given by $\boldsymbol{U}_1 = \boldsymbol{U}_1^{+} + \boldsymbol{U}_1^{-}$. The result is obtained by adding respectively (4.5), (4.6) and (4.7), to (4.13), (4.14) and (4.15). Taking the real part of the resulting fields, we get

$$\Psi_{11}(r, \theta, t) = 0, \tag{4.16}$$

$$\Phi_{21}(r, \theta, t) = \tfrac{1}{2}\omega r^2 \sin(\omega t), \tag{4.17}$$

$$\Psi_{21}(r, \theta, t) = \left(r^2\Omega - \frac{\Gamma}{2\pi}\right)\cos(\omega t) + 2g_{2,\omega}(r)\cos(2\theta - \omega t) + 2g_{-2,\omega}(r)\cos(2\theta + \omega t). \tag{4.18}$$

As expected, $\boldsymbol{U}_{11}(\boldsymbol{x}, t) = 0$ (everywhere), so that the motion of translation is annihilated by superposing the second wave.

4.4. *Parametric resonances in the vortex core*

The behaviour of the field

$$\boldsymbol{U}_{21} = \nabla\Phi_{21} + \boldsymbol{e}_z \times \nabla\Psi_{21} \tag{4.19}$$

may be evaluated at $r = 0$ without knowing exactly the functions $g_{2,\omega}(r)$ and $g_{-2,\omega}(r)$, since their behaviour when $r \to 0$ is easily shown to be (Drazin & Reid 1981):

$$g_{\pm 2,\omega}(r) \sim A_{\pm 2} r^2, \tag{4.20}$$

except when the critical layer is located at the origin (Bassom & Gilbert 1998). But this case has been excluded here, by imposing the condition (4.9). $A_{\pm 2}$ are real numbers depending on ω, that have to be determined from the general solution of the Rayleigh equation (4.8). From (4.17) and (4.18), this is however sufficient to conclude that $\boldsymbol{U}_{21} = 0$ at $r = 0$, so that at $O(\delta \mathcal{M}^2)$, the core of the vortex is a stagnation point.

Let us now evaluate the velocity gradient tensor of the flow in the vortex core $\boldsymbol{x}_0 = 0$. Expressing the result in Cartesian coordinates, we get

$$\boldsymbol{L}(\boldsymbol{x}_0, t) = \boldsymbol{L}_0 + \delta \mathcal{M}^2 \boldsymbol{L}_{21}(t) + O(\delta^2), \tag{4.21}$$

with

$$\boldsymbol{L}_0 = \frac{1}{2}\begin{pmatrix} 0 & -1 \\ 1 & 0 \end{pmatrix}, \tag{4.22}$$

and

$$\boldsymbol{L}_{21}(t) = \begin{pmatrix} \omega \sin(\omega t) & -\cos(\omega t) \\ \cos(\omega t) & \omega \sin(\omega t) \end{pmatrix} + \begin{pmatrix} \alpha \sin(\omega t) & \beta \cos(\omega t) \\ \beta \cos(\omega t) & -\alpha \sin(\omega t) \end{pmatrix}, \tag{4.23}$$

where $\alpha = 4(A_{-2} - A_2)$ and $\beta = 4(A_2 + A_{-2})$. The first term on the right-hand side of (4.23) may be recognized as a pure circular compression effect, see (3.6). The second is an irrotational periodic straining field, which may occur in incompressible flows: the second term in the right-hand side of (3.16) is recovered with $\alpha = \omega/2$ and $\beta = \frac{1}{2}$; the case $\alpha = \beta$ corresponds to a circular vortex in a rotating strain (Le Dizès 2000*a*, *b*); and the case $\alpha = 0$ has been solved by Craik & Allen (1992) for an incompressible rotating column of fluid.

At order $\delta \mathcal{M}^2$, the stability properties of the vortex core under the effect of the waves will be given by solving the Hill–Schrödinger equation

$$\frac{\mathrm{d}^2 q}{\mathrm{d}t^2} + \{Q_0 + \delta \mathcal{M}^2 Q_{21}(t)\} q = 0, \tag{4.24}$$

where $Q_0 = \mu^2$ and $Q_{21}(t)$ is given by

$$\begin{aligned} Q_{21}(t) = {} & 2\mu^2 \left(\mu^2 + 1 - \frac{\omega^2}{2}\right) \cos(\omega t) \\ & + 16\mu^2 \frac{A_{-2}}{1+\omega} \left(\frac{\mu^2}{2} - \frac{\omega^2 + 5}{4} - \omega\right) \cos(1+\omega)t \\ & + 16\mu^2 \frac{A_2}{1-\omega} \left(\frac{\mu^2}{2} - \frac{\omega^2 + 5}{4} + \omega\right) \cos(1-\omega)t. \end{aligned} \tag{4.25}$$

Again we obtain here an almost-periodic potential when ω is irrational, but to order $\delta \mathcal{M}^2$ the first parametric resonances may be completely determined by a multiple-scale analysis, as performed previously. Details of the calculations are omitted for brevity.

Since $\omega > 0$ and $0 < \mu < 1$, it is clear that instability cannot happen unless

$$0 < \omega < 3. \tag{4.26}$$

The first resonance arises when $0 < \omega < 2$ and corresponds to the pure compression term of the flow, i.e. the first term on the right-hand side of (4.25): the perturbation grows exponentially with growth rate

$$\sigma = \delta \mathscr{M}^2 \frac{\omega}{4}\left(1 - \frac{\omega^2}{4}\right). \tag{4.27}$$

The two following resonances arise from the irrotational straining part of the flow. One of them exists when $0 < \omega < 1$, and the growth rate of the instabilities is given by

$$\sigma = \delta \mathscr{M}^2 \frac{|A_{-2}|}{4}(\omega + 3)^2. \tag{4.28}$$

Finally, the last resonance arises when $0 < \omega < 3$, with growth rate:

$$\sigma = \delta \mathscr{M}^2 \frac{|A_2|}{4}(\omega - 3)^2. \tag{4.29}$$

Thus, without knowing exactly the values of $A_{\pm 2}$, we may first conclude that a vortex with two incident waves is always unstable to three-dimensional short-wavelength instabilities when $0 < \omega < 2$, since (4.27) is independent of $A_{\pm 2}$, and thus independent of the velocity distribution in the vortex. Furthermore, it is clear that in a smooth vortex, we expect that $A_{\pm 2} \neq 0$, so that both instabilities described by (4.28) and (4.29) should occur respectively when $0 < \omega < 1$ and $0 < \omega < 3$. If ω is in a range where various resonances occur, the most amplified instability will dominate of course.

4.5. *Application to a Rankine vortex*

For a Rankine vortex, i.e. the potential vortex outside a core of finite circular size and constant vorticity, corrections coming from the interaction of acoustic waves may be completely determined. The vortex is defined in dimensionless form by

$$\Omega(r) = \begin{cases} \frac{1}{2}, & r < 1 \\ r^{-2}/2, & r > 1, \end{cases} \tag{4.30}$$

so that the core radius and vorticity are unity.

As shown in Appendix B (see also Saffman 1992), and providing that

$$\omega \neq \tfrac{1}{2}, \quad \omega \neq 1, \tag{4.31}$$

the functions $g_{\pm 2,\omega}(r)$, solutions of the radial Rayleigh equation, may be calculated explicitly, and are given by

$$g_{\pm 2,\omega}(r) = \begin{cases} A_{\pm 2} r^2, & r < 1 \\ B_{\pm 2} r^{-2} + C_{\pm 2} r^2, & r > 1, \end{cases} \tag{4.32}$$

where $C_{\pm 2}$ are constants that are determined from matching conditions with the outer solution when $r \to \infty$. They are given by $C_2 = -\omega/8$ and $C_{-2} = \omega/8$ (Ford & Llewellyn Smith 1999). As a consequence, we get from Appendix B

$$A_2 = -\frac{\omega}{4}\frac{\omega - 1}{2\omega - 1}, \quad A_{-2} = \frac{\omega}{4}\frac{\omega + 1}{2\omega + 1}. \tag{4.33}$$

The values of $B_{\pm 2}$ may be deduced from the relation $A_{\pm 2} = B_{\pm 2} + C_{\pm 2}$ (Appendix B).

Recall that the resonance $0 < \omega < 2$ corresponding to the pure compression effect is universal and insensitive to the vorticity distribution, since (4.27) is independent of

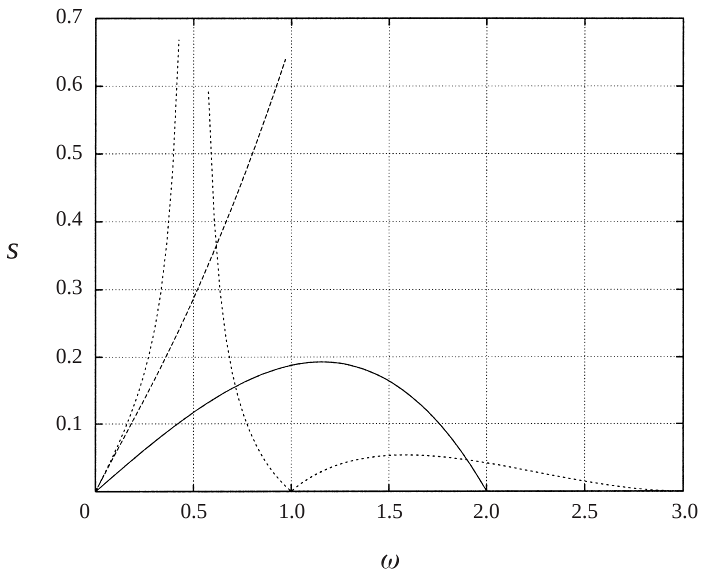

FIGURE 4. Rescaled growth rates $s = \sigma/(\delta\mathscr{M}^2)$ of the various principal parametric instabilities for a Rankine vortex with two opposite incident waves, given by (4.27), (4.34) and (4.35). Note that (4.35) diverges at $\omega = \frac{1}{2}$.

$A_{\pm 2}$. On the other hand, the growth rates (4.28) and (4.29) of the straining resonances are now respectively, taking (4.33) into account,

$$\sigma = \delta\mathscr{M}^2 \frac{\omega}{16}\left|\frac{\omega+1}{2\omega+1}\right|(\omega+3)^2, \tag{4.34}$$

valid when $0 < \omega < 1$, and

$$\sigma = \delta\mathscr{M}^2 \frac{\omega}{16}\left|\frac{\omega-1}{2\omega-1}\right|(\omega-3)^2, \tag{4.35}$$

valid when $0 < \omega < 3$. The interactions between resonances arising when $\omega = \frac{1}{2}$ or $\omega = 1$ are excluded (see Appendix B). Results are plotted on figure 4.

5. Discussion and conclusion

The geometrical optics stability theory elaborated by Eckhoff (1981) and Lifschitz & Hameiri (1991) has been used to show the existence of short-wavelength three-dimensional parametric instabilities in time-periodic circular vortex cores of an inviscid ideal gas.

The most important application of the present results is that a circular vortex may be destabilized by a couple of plane acoustic waves with long wavelength, propagating in opposite directions. Based on the asymptotic solution of Ford & Llewellyn Smith (1999) for a single wave, it has been proved that the superposition of two waves leaves the position the vortex core steady, and perturbs the vortex locally by pure circular compressions and irrotational strains. For a smooth vortex with unit core vorticity, the pure compression part of the perturbation gives rise to a universal parametric resonance when $0 < \omega < 2$, with growth rate independent of the velocity distribution in the vortex. The straining field operates generally when $0 < \omega < 3$, but the growth rate now depends on the structure of the vortex. In the case of a Rankine vortex, characterization of the various resonances has been carried out. In each case, the growth rates scale with $\delta \mathscr{M}^2$, where δ is the dimensionless wave amplitude, and $\mathscr{M}$ the characteristic Mach number of the vortex.

In a medium at rest, Broadbent & Moore (1979) showed that a Rankine vortex is unstable to two-dimensional acoustic modes, with growth rates scaling as $\mathscr{M}^4$, so that the three-dimensional parametric resonances may be more dangerous, providing that $\delta > \mathscr{M}^2$. In an incompressible framework, the stability of a Rankine vortex subjected to steady external strains has been determined by normal mode methods (Tsai & Widnall 1976; Eloy & Le Dizès 2000). As expected, the resulting growth rates at large wavenumber converge to the value given by the geometrical optics stability theory (Le Dizès & Eloy 1999), a situation encountered in many other circumstances (Leibovich & Stewartson 1983; Bayly 1988; Sipp *et al.* 1999; Le Duc & Leblanc 1999). In the present case, a normal mode approach could be used to explore the stability of compressed vortices. However, the situation is much more complex here because difficulties arise from the fact that the basic flow is compressible and unsteady. Viscosity has not been taken into account in the present analysis. In an unbounded flow, viscosity is responsible for a pure volumic effect which leads to a small damping of the instabilities, providing that the Reynolds number is sufficiently high.

To our knowledge, the three-dimensional destabilization of a vortex by acoustic waves has never been observed, neither experimentally nor numerically. Generally, the vortex interacts with a single acoustic wave, and measurements of scattered acoustic fields are performed with various experimental techniques (Lund & Rojas 1989; Dernoncourt *et al.* 1998; Labbé & Pinton 1998; Oljaca *et al.* 1998; Manneville *et al.* 1999). From the results derived in the present study, it is not obvious that a single wave may destabilize a vortex since the vortex core moves periodically, so that the vortex core is no longer a stagnation point. Nevertheless, and to conclude, we might imagine interesting applications of the mechanisms of parametric resonance exposed here, such as the destabilization of strong cyclonic atmospheric vortices by a pair of acoustic waves.

I am particularly grateful to A. Le Duc for very stimulating exchanges about short-wavelength instabilities in compressible flows. Constructive criticisms of the anonymous Referees are also greatly acknowledged. This work has been partly carried out at Ecole Centrale de Lyon, and has benefited from discussions with L. Le Penven and J. Scott.

Appendix A. Parametric instabilities for axial compressions

A.1. *Conditions of resonances*

We look for the solution of (3.19) with $Q_0 = \mu^2$ and $Q_1(t)$ given by (3.18). The solution is sought in the multiple-scale form (Bender & Orszag 1978):

$$q(\boldsymbol{x}_0, t) = q_0(t, \tau) + \delta q_1(t, \tau) + O(\delta^2), \quad \tau = \delta t, \tag{A 1}$$

where τ is a slow time scale. Suppose that a resonance occurs when $\mu = \mu_0$. Near this resonance, we have

$$\mu = \mu_0 + \delta \mu_1 + O(\delta^2). \tag{A 2}$$

From (3.18), we get, up to order δ,

$$\frac{\partial^2 q_0}{\partial t^2} + \mu_0^2 q_0 = 0, \tag{A 3}$$

$$\frac{\partial^2 q_1}{\partial t^2} + \mu_0^2 q_1 = -2\frac{\partial^2 q_0}{\partial t \partial \tau} - 2\mu_0\mu_1 q_0 - Q_1 q_0. \tag{A 4}$$

The solution of (A 3) is

$$q_0(t,\tau) = A(\tau)\mathrm{e}^{\mathrm{i}\mu_0 t} + \text{c.c.}, \tag{A 5}$$

and the forcing terms on the right-hand side of (A 4) are respectively

$$2\frac{\partial^2 q_0}{\partial t \partial \tau} + 2\mu_0\mu_1 q_0 = 2\mu_0\left(\mathrm{i}\frac{\mathrm{d}A}{\mathrm{d}\tau} + \mu_1 A\right)\mathrm{e}^{\mathrm{i}\mu_0 t} + \text{c.c.}, \tag{A 6}$$

and

$$\begin{aligned} Q_1 q_0 = \frac{\mu_0^2}{2} A \Bigg\{ & \left(1 + \mu_0^2 - \frac{\omega^2}{2}\right)\left(\mathrm{e}^{\mathrm{i}(\mu_0+\omega)t} + \mathrm{e}^{\mathrm{i}(\mu_0-\omega)t}\right) \\ & + \left(\frac{\mu_0^2}{2} - \frac{\omega^2+5}{4} - \omega\right)\left(\mathrm{e}^{\mathrm{i}(\mu_0+\omega+1)t} + \mathrm{e}^{\mathrm{i}(\mu_0-\omega-1)t}\right) \\ & + \left(\frac{\mu_0^2}{2} - \frac{\omega^2+5}{4} + \omega\right)\left(\mathrm{e}^{\mathrm{i}(\mu_0-\omega+1)t} + \mathrm{e}^{\mathrm{i}(\mu_0+\omega-1)t}\right)\Bigg\} + \text{c.c.} \end{aligned} \tag{A 7}$$

Thus the solution of (A 4) is bounded except for various resonances arising when the arguments of the complex exponential terms in (A 7) are identical to μ_0, corresponding to the homogeneous solution (A 5). Taking into account that $0 < \mu < 1$ and $\omega > 0$, the various conditions for resonance are

$$\omega = 2\mu_0, \quad 1 \pm \omega = 2\mu_0, \quad \omega - 1 = 2\mu_0. \tag{A 8}$$

Inside those bands, some particular cases may arise that correspond to interaction between various bands. Some details are given below.

We recall that the case $\mu = 0$ (two-dimensional perturbations) is stable. The case $\mu = 1$ (spanwise wave vectors) which requires a special analysis is also studied. Since $\tau = \delta t$, note that the growth rates s given below have to be multiplied by δ to get the physical growth rates: $\sigma = \delta s$.

A.2. *General resonances*

Case $\omega = 2\mu_0$, *with* $\mu_0 \neq \frac{1}{2}$ *and* $\mu_0 \neq \frac{1}{4}$. Elimination of secular terms yields the following amplitude equation:

$$\frac{\mathrm{d}A}{\mathrm{d}\tau} = \mathrm{i}(\mu_1 A + sA^*), \quad s = \frac{\omega}{8}\left(1 - \frac{\omega^2}{4}\right), \tag{A 9}$$

the linearly independent solutions of which are

$$A^{\pm}(\tau) = \exp\{\pm\tau(s^2 - \mu_1^2)^{1/2}\}. \tag{A 10}$$

Exponential instability occurs when $|\mu_1| < |s|$. The maximum growth rate s is reached when $\mu_1 = 0$ and $0 < \omega < 2$. This case is similar to the circular compressions.

Case $1 \pm \omega = 2\mu_0$ *with* $\mu_0 \neq \frac{1}{4}$. The amplitude equations are

$$\frac{\mathrm{d}A}{\mathrm{d}\tau} = \mathrm{i}(\mu_1 A - s^{\pm}A^*), \quad s^{\pm} = \frac{1}{64}(1 \pm \omega)(3 \pm \omega)^2. \tag{A 11}$$

Exponential instabilities occur when $|\mu_1| < |s|$. The maximum growth rates $s^{\pm}$ are reached when $\mu_1 = 0$ and $0 < \omega < 1$.

Case $\omega - 1 = 2\mu_0$. The amplitude equation is

$$\frac{\mathrm{d}A}{\mathrm{d}\tau} = \mathrm{i}(\mu_1 A - sA^*), \quad s = \frac{1}{64}(\omega-1)(\omega-3)^2. \tag{A 12}$$

Exponential instability occurs when $|\mu_1| < |s|$. The maximum growth rate s is reached when $\mu_1 = 0$ and $1 < \omega < 3$.

A.3. *Particular cases*

Case $\omega = \frac{1}{2}$ *and* $\mu_0 = \frac{1}{4}$. This is a manifestation of the interaction between two of the resonances described above: $\omega = 2\mu_0$ and $1-\omega = 2\mu_0$. In this case, the secular terms vanish when the envelope satisfies

$$\frac{\mathrm{d}A}{\mathrm{d}\tau} = \mathrm{i}\left(\mu_1 A + \frac{5}{512}A^*\right). \tag{A 13}$$

Exponential instability occurs when $|\mu_1| < \frac{5}{512}$. The maximum growth rate

$$s = \frac{5}{512} \tag{A 14}$$

is reached when $\mu_1 = 0$. Then we can see that the growth rates obtained previously for the resonances $\omega = 2\mu_0$ and $1-\omega = 2\mu_0$ are discontinuous when $\omega = \frac{1}{2}$.

Case $\omega = 1$ *and* $\mu_0 = \frac{1}{2}$. This case is very particular, because the amplitude equation is

$$\frac{\mathrm{d}A}{\mathrm{d}\tau} = \mathrm{i}\left\{\frac{3}{32}(A^* - A) + \mu_1 A\right\}, \tag{A 15}$$

the linearly independent solutions of which are

$$A^{\pm}(\tau) = \exp\left\{\pm\tau\sqrt{\mu_1}\left(\frac{3}{16} - \mu_1\right)^{1/2}\right\}. \tag{A 16}$$

Exponential instability occurs when $0 < \mu_1 < \frac{3}{16}$. The maximum growth rate

$$s = \frac{3}{32} \tag{A 17}$$

is reached for $\mu_1 = 3/32$. Note that this growth rate matches the growth rate obtained for $\omega = 2\mu_0$ when $\omega \to 1$.

A.4. *Spanwise wave vectors*

When $\mu = 1$, the Hill–Schrödinger equation is formally no longer valid. Nevertheless, following the treatment by Leblanc & Le Penven (1999), this case may be also studied by noting that the transport equation reduces to a 2×2 system independent of the wave vector:

$$\frac{\mathrm{d}\tilde{\boldsymbol{v}}}{\mathrm{d}t} = -\boldsymbol{L}\,\tilde{\boldsymbol{v}}, \tag{A 18}$$

where $\tilde{\boldsymbol{v}}(\boldsymbol{x}_0, t)$ is the projection of $\sqrt{R}\boldsymbol{a}$ on the $(\boldsymbol{e}_x, \boldsymbol{e}_y)$-plane.

This system may be reduced to a single equation by taking the time derivative for the first component $\tilde{u} = \tilde{\boldsymbol{v}} \cdot \boldsymbol{e}_x$. To order δ, this yields the single equation

$$\frac{\mathrm{d}^2\tilde{u}}{\mathrm{d}t^2} + \delta\omega\sin(\omega t)\frac{\mathrm{d}\tilde{u}}{\mathrm{d}t} + \left\{\tfrac{1}{4} + \delta\left(\tfrac{1}{2} + \omega^2\right)\cos(\omega t)\right\}\tilde{u} = 0, \tag{A 19}$$

which may be studied directly by a standard multiple-scale analysis, or by noting that it may be rewritten in the standard Hill form with a suitable change of variables.

Indeed,

$$\frac{\mathrm{d}^2\tilde{u}}{\mathrm{d}t^2} + a\frac{\mathrm{d}\tilde{u}}{\mathrm{d}t} + b\tilde{u} = 0, \tag{A 20}$$

may be transform into

$$\frac{\mathrm{d}^2\tilde{q}}{\mathrm{d}t^2} + Q(\boldsymbol{x}_0, t)\tilde{q} = 0, \tag{A 21}$$

by the following change of variables (Magnus & Winkler 1966):

$$\tilde{q} = \mathrm{e}^{A/2}\tilde{u}, \quad a = \frac{\mathrm{d}A}{\mathrm{d}t}, \quad Q = -\frac{1}{2}\frac{\mathrm{d}a}{\mathrm{d}t} - \frac{a^2}{4} + b, \tag{A 22}$$

giving, in our case,

$$Q(\boldsymbol{x}_0, t) = \tfrac{1}{4} + \tfrac{1}{2}\delta(\omega^2 + 1)\cos(\omega t) + O(\delta^2). \tag{A 23}$$

Clearly, from the theory of parametric resonance, or by a standard multiple-scale analysis (Bender & Orszag 1978), solutions are periodic, except near the first resonance $\omega = 1$ for which the solution grows exponentially with growth rate

$$\sigma = \delta/2. \tag{A 24}$$

This growth rate matches the one obtained previously in the case $1 + \omega = 2\mu$ when $\mu \to 1$. This result is in accordance with the analysis of Leblanc & Le Penven (1999) who showed that this resonance also occurs when compressing periodically an elliptical vortex.

Appendix B. Solution of Rayleigh equation for the Rankine vortex

B.1. *Jump conditions*

The Rankine vortex presents a discontinuous distribution of vorticity, so that solution of the Rayleigh equation has to satisfy jump conditions at the interface $r = 1$. For an incompressible inviscid fluid, the linear two-dimensional modes $[\hat{u}, \hat{v}, \hat{p}](r)\exp \mathrm{i}(n\theta - \omega t)$ are solutions of the system (Drazin & Reid 1981; Saffman 1992)

$$\mathrm{i}(n\Omega - \omega)\hat{u} - 2\Omega\hat{v} = -\mathrm{d}\hat{p}/\mathrm{d}r, \tag{B 1}$$

$$\mathrm{i}(n\Omega - \omega)\hat{v} + W\hat{u} = -\mathrm{i}n\hat{p}/r, \tag{B 2}$$

$$\mathrm{d}\hat{u}/\mathrm{d}r + \hat{u}/r + \mathrm{i}n\hat{v}/r = 0. \tag{B 3}$$

For a homentropic flow, using dimensionless variables similar to those of Ford & Llewellyn Smith (1999), density satisfies $\hat{\varrho}(r) = \gamma C^2\hat{p}(r)$.

With $\hat{\psi}(r)$ defined by $\hat{u} = -\mathrm{i}n\hat{\psi}/r$ and $\hat{v} = \mathrm{d}\hat{\psi}/\mathrm{d}r$, continuity of pressure at the interface gives

$$\left[r(n\Omega - \omega)\frac{\mathrm{d}\hat{\psi}}{\mathrm{d}r} - nW\hat{\psi}\right]^{\pm} = 0, \tag{B 4}$$

where $[f(r)]^{\pm} = f(r \to 1^+) - f(r \to 1^-)$.

The interface being a material line, it may be shown that continuity of radial velocity at the deformed interface implies

$$\left[\frac{\hat{\psi}}{n\Omega - \omega}\right]^{\pm} = 0. \tag{B 5}$$

B.2. *Solution of the Rayleigh equation*

It remains to solve Rayleigh equation (4.8) for $\hat{\varphi}(r)$ on each side of the interface for Rankine solution (4.30). Since the vorticity is constant, the critical layer r_0 such that $n\Omega(r_0) = \omega$ is regular, and the general solution is:

$$\hat{\varphi}(r) = \begin{cases} Ar^n, & r < 1 \\ Br^{-n} + Cr^n, & r > 1. \end{cases} \tag{B 6}$$

When $\omega \neq n/2$, jump conditions (B 4) and (B 5) imply

$$A - B = C, \quad A\left(1 - \frac{2\mathrm{sgn}(n)}{n - \mathrm{sgn}(n) - 2\omega}\right) + B = C. \tag{B 7}$$

When $C = 0$ (no strain at infinity), the solution given for instance by Saffman (1992) is recovered. System (B 7) admits a non-trivial solution when $2\omega \neq n - \mathrm{sgn}(n)$. It is

$$A = \frac{n - 2\omega}{n - \mathrm{sgn}(n) - 2\omega} C, \quad B = \frac{\mathrm{sgn}(n)}{n - \mathrm{sgn}(n) - 2\omega} C. \tag{B 8}$$

We assume here that C is given by conditions on $\hat{\varphi}(r)$ when $r \to \infty$.

REFERENCES

Bassom, A. P. & Gilbert, A. D. 1998 The spiral wind-up of vorticity in an inviscid planar vortex. *J. Fluid Mech.* **371**, 109–140.

Bayly, B. J. 1988 Three-dimensional centrifugal-type instabilities in inviscid two-dimensional flows. *Phys. Fluids* **31**, 56–64.

Bayly, B. J., Holm, D. D. & Lifschitz, A. 1996 Three-dimensional stability of elliptical vortex columns in external strain flows. *Phil. Trans. R. Soc. Lond.* A **354**, 895–926.

Bender, C. M. & Orszag, S. A. 1978 *Advanced Mathematical Methods for Scientists and Engineers.* McGraw-Hill.

Broadbent, E. G. & Moore, D. W. 1979 Acoustic destabilization of vortices. *Phil. Trans. R. Soc. Lond.* A **290**, 353–371.

Chagelishvili, G. D., Khujadze, G. R., Lominadze, J. G. & Rogava, A. D. 1997 Acoustic waves in unbounded shear flows. *Phys. Fluids* **9**, 1955–1962.

Colonius, T., Lele, S. K. & Moin, P. 1994 The scattering of sound waves by a vortex: numerical simulations and analytical solutions. *J. Fluid Mech.* **260**, 271–298.

Craik, A. D. D. & Allen, H. R. 1992 The stability of three-dimensional time-periodic flows with spatially uniform strain rates. *J. Fluid Mech.* **234**, 613–628.

Dernoncourt, B., Pinton, J.-F. & Fauve, S. 1998 Experimental study of vorticity filaments in a turbulent swirling flow. *Physica* D **117**, 181–190.

Dobrokhotov, S. Yu. & Shafarevich, A. I. 1992 Parametrix and asymptotics of localized solutions of the Navier–Stokes equations in $\mathscr{R}^3$, linearized on a smooth flow. *Mat. Zametki* (*Math. Notes*) **51**, 72–82.

Drazin, P. G. & Reid, W. H. 1981 *Hydrodynamic Stability*. Cambridge.

Eckhoff, K. S. 1981 On stability for symmetric hyperbolic systems, I. *J. Diffl Equat.* **40**, 94–115.

Eckhoff, K. S. 1984 A note on the instability of columnar vortices. *J. Fluid Mech.* **145**, 417–421.

Eckhoff, K. S. & Storesletten, L. 1978 A note on the stability of steady inviscid helical gas flows. *J. Fluid Mech.* **89**, 401–411.

Eckhoff, K. S. & Storesletten, L. 1980 On the stability of rotating compressible and inviscid fluids. *J. Fluid Mech.* **99**, 433–448.

Eloy, C. & Le Dizès, S. 2000 Stability of Rankine vortex in a multipolar strain field. Submitted to *Phys. Fluids.*

Fabijonas, B., Holm, D. D. & Lifschitz, A. 1997 Secondary instabilities of flows with elliptic streamlines. *Phys. Rev. Lett.* **78**, 1900–1903.

Ford, R. & Llewellyn Smith, S. G. 1999 Scattering of acoustic waves by a vortex. *J. Fluid Mech.* **386**, 305–328.

Friedlander, S. & Vishik, M. M. 1991 Instability criteria for the flow of an inviscid incompressible fluid. *Phys. Rev. Lett.* **66**, 2204–2206.

Friedlander, S. & Vishik, M. M. 1992 Instability criteria for steady flows of a perfect fluid. *Chaos* **2**, 455–460.

Gans, R. F. 1975 On the stability of shear flow in a rotating gas. *J. Fluid Mech.* **68**, 403–412.

Ho, C.-M. & Huerre, P. 1984 Perturbed free shear layers. *Ann. Rev. Fluid Mech.* **16**, 365–424.

Huerre, P. & Rossi, M. 1998 Hydrodynamic instabilities in open flows. In *Hydrodynamics and Nonlinear Instabilities* (ed. C. Godrèche & P. Manneville), pp. 81–294. Cambridge University Press.

Kraichnan, R. H. 1953 The scattering of sound in a turbulent medium. *J. Acoust. Soc. Am.* **25**, 1096–1104.

Labbé, R. & Pinton, J.-F. 1998 Propagation of sound through a turbulent vortex. *Phys. Rev. Lett.* **81**, 1413–1416.

Lalas, D. P. 1975 The 'Richardson' criterion for compressible swirling flows. *J. Fluid Mech.* **69**, 65–72.

Landau, L. D. & Lifshitz, E. M. 1959 *Fluid Mechanics*. Pergamon.

Leblanc, S. 1997 Stability of stagnation points in rotating flows. *Phys. Fluids* **9**, 3566–3569.

Leblanc, S. & Cambon, C. 1998 Effects of the Coriolis force on the stability of Stuart vortices. *J. Fluid. Mech.* **356**, 353–379.

Leblanc, S. & Le Penven, L. 1999 Stability of periodically compressed vortices at low Mach number. *Phys. Fluids* **11**, 955–957.

Lebovitz, N. & Lifschitz, A. 1992 Short wavelength instabilities of rotating, compressible fluid masses. *Proc. R. Soc. Lond.* A **438**, 265–290.

Lebovitz, N. R. & Lifschitz, A. 1996 Short-wavelength instabilities of Riemann ellipsoids. *Phil. Trans. R. Soc. Lond.* A **354**, 927–950.

Le Dizès, S. 2000*a* Non-axisymmetric vortices in two-dimensional flows. *J. Fluid Mech.* **406**, 175–198.

Le Dizès, S. 2000*b* Three-dimensional instability of a multipolar vortex in a rotating flow. Submitted to *Phys. Fluids.*

Le Dizès, S. & Eloy, C. 1999 Short-wavelength instability of a vortex in a multipolar strain field. *Phys. Fluids* **11**, 500–502.

Le Duc, A. & Leblanc, S. 1999 A note on Rayleigh stability criterion for compressible flows. *Phys. Fluids* **11**, 3563–3566.

Leibovich, S. & Stewartson, K. 1983 A sufficient condition for the instability of columnar vortices. *J. Fluid Mech.* **126**, 335–356.

Lifschitz, A. E. 1989 *Magnetohydrodynamics and Spectral Theory*. Kluwer.

Lifschitz, A. 1991 Essential spectrum and local stability condition in hydrodynamics. *Phys. Lett.* A **152**, 199–204.

Lifschitz, A. 1994 On the instability of certain motions of an ideal incompressible fluid. *Adv. Appl. Math.* **15**, 404–436.

Lifschitz, A. & Hameiri, E. 1991 Local stability conditions in fluid dynamics. *Phys. Fluids* A **3**, 2644–2651.

Lifschitz, A. & Hameiri, E. 1993 Localized instabilities of vortex rings with swirl. *Commun. Pure Appl. Maths* **46**, 1379–1408.

Lighthill, M. J. 1953 On the energy scattered from the interaction of turbulence with sound or shock waves. *Proc. Camb. Phil. Soc.* **49**, 537–551.

Lund, F. & Rojas, C. 1989 Ultrasound as a probe of turbulence. *Physica* D **37**, 508–514.

Magnus, W. & Winkler, S. 1966 *Hill's Equation*. Wiley.

Manneville, S., Robres, J. H., Maurel, A., Petitjeans, P. & Fink, M. 1999 Vortex dynamics investigation using an acoustic technique. *Phys. Fluids* **11**, 3380–3389.

Mansour, N. N. & Lundgren, T. S. 1990 Three-dimensional instability of rotating flows with oscillating axial strain. *Phys. Fluids* A **2**, 2089–2091.

Miyazaki, T. & Adachi, K. 1998 Short-wavelength instabilities of waves in rotating stratified fluids. *Phys. Fluids* **10**, 3168–3177.

Moore, D. W. & Pullin, D. I. 1998 On steady compressible flows with compact vorticity; the compressible Hill's spherical vortex. *J. Fluid Mech.* **374**, 285–303.

Moore, D. W. & Saffman, P. G. 1975 The instability of a straight vortex filament in a strain field. *Proc. R. Soc. Lond.* A **346**, 413–425.

Oljaca, M., Gu, X., Glezer, A., Baffico, M. & Lund, F. 1998 Ultrasound scattering by a swirling jet. *Phys. Fluids* **10**, 886–898.

Reinschke, J., Möhring, W. & Obermeier, F. 1997 Scattering of sound waves by a cylindrical vortex: a semi-analytical theory. *J. Fluid Mech.* **333**, 273–299.

Reyl, C., Antonsen, T. M. Jr. & Ott, E. 1997 Nature of the vorticity field generated by instabilities of chaotic fluid flows. *Phys. Rev. Lett.* **78**, 2559–2562.

Saffman, P. G. 1992 *Vortex Dynamics*. Cambridge University Press.

Simone, A., Coleman, G. N. & Cambon, C. 1997 The effect of compressibility on turbulent shear flow: a rapid-distortion-theory and direct-numerical-simulation study. *J. Fluid Mech.* **330**, 307–338.

Sipp, D. & Jacquin, L. 1998 Elliptic instability in two-dimensional flattened Taylor–Green vortices. *Phys. Fluids* **10**, 839–849.

Sipp, D. & Jacquin, L. 2000 Three-dimensional centrifugal-type instabilities of two-dimensional flows in rotating systems. *Phys. Fluids* (to appear).

Sipp, D., Lauga, E. & Jacquin, L. 1999 Vortices in rotating systems: Centrifugal, elliptic and hyperbolic type instabilities. *Phys. Fluids* **11**, 3716–3728.

Tsai, C.-Y. & Widnall, S. E. 1976 The stability of short waves on a straight vortex filament in a weak externally imposed strain field. *J. Fluid Mech.* **73**, 721–733.

Vishik, M. M. & Friedlander, S. 1993 Dynamo theory methods for hydrodynamic stability. *J. Math. Pures Appl.* **72**, 145–180.

Warren, F. W. 1975 A comment on Gans' stability criterion for steady inviscid helical gas flows. *J. Fluid Mech.* **68**, 413–415.